Title

Screening and functional identification of lncRNAs under β-diketone antibiotic exposure to zebrafish (Danio rerio) using high-throughput sequencing

Authors

Wang, Xuedong
Lin, Jiebo
Li, Fanghui
et al.

Publication Date

2017

DOI

10.1016/j.aquatox.2016.12.003

Peer reviewed

Aquatic Toxicology 182 (2017) 214–225

Contents lists available at ScienceDirect

Aquatic Toxicology

journal homepage: www.elsevier.com/locate/aquatox

Screening and functional identification of lncRNAs under β-diketone antibiotic exposure to zebrafish (*Danio rerio*) using high-throughput sequencing

Xuedong Wang[a], Jiebo Lin[b], Fanghui Li[b], Cao Zhang[b,**], Jieyi Li[b], Caihong Wang[b], Randy A. Dahlgren[a], Hongqin Zhang[b,*], Huili Wang[b,*]

[a] Key Laboratory of Watershed Sciences and Health of Zhejiang Province, Wenzhou Medical University, Wenzhou 325035, China
[b] College of Life Sciences, Wenzhou Medical University, Wenzhou 325035, China

ARTICLE INFO

Article history:
Received 16 October 2016
Received in revised form
30 November 2016
Accepted 2 December 2016
Available online 5 December 2016

Keywords:
Long non-coding RNAs (lncRNAs)
β-Diketone antibiotics (DKAs)
High-throughput sequencing
In situ hybridization (ISH)
lncRNA-regulating target genes
Histopathological observation

ABSTRACT

Long non-coding RNAs (lncRNAs) have attracted considerable research interest, but so far no data are available on the roles of lncRNAs and their target genes under chronic β-diketone antibiotic (DKAs) exposure to zebrafish (*Danio rerio*). Herein, we identified 1.66, 3.07 and 3.36 × 10^4 unique lncRNAs from the 0, 6.25 and 12.5 mg/L DKA treatment groups, respectively. In comparison with the control group, the 6.25 and 12.5 mg/L treatments led to up-regulation of 2064 and 2479 lncRNAs, and down-regulation of 778 and 954 lncRNAs, respectively. Of these, 44 and 39 lncRNAs in the respective 6.25 and 12.5 mg/L treatments displayed significant differential expression. Volcano and Venn diagrams of the differentially expressed lncRNAs were constructed on the basis of the differentially expressed lncRNAs. After analyzing 10 lncRNAs and potential target genes, a complex interaction network was constructed between them. The consistency of 7 target genes (*tenm3*, *smarcc1b*, *myo9ab*, *ubr4*, *hoxb3a*, *mycbp2* and *CR388046.3*), co-regulated by 3 lncRNAs (TCONS_00129029, TCONS_00027240 and TCONS_00017790), was observed between their qRT-PCR and transcriptomic sequencing. By *in situ* hybridization (ISH), abnormal expression of 3 lncRNAs was observed in hepatic and spleen tissues, suggesting that they might be target organs for DKAs. A similar abnormal expression of two immune-related target genes (*plk3* and *syt10*), co-regulated by the 3 identified lncRNAs, was observed in liver and spleen by ISH. Histopathological observations demonstrated hepatic parenchyma vacuolar degeneration and clot formation in hepatic tissues, and uneven distribution of brown metachromatic granules and larger nucleus in spleen tissues resulting from DKA exposure. Overall, DKA exposure led to abnormal expression of some lncRNAs and their potential target genes, and these genes might play a role in immune functions of zebrafish.

1. Introduction

Long non-coding RNAs (lncRNAs) are a recently discovered class of non-protein-coding transcripts encoded by many metazoan genomes (Soshnev et al., 2011). Members of this class have been annotated in recent years following transcriptome annotation of metazoans using deep sequencing approaches (Yan et al., 2012). By definition, lncRNAs are transcripts with a length of more than 200 nucleotides and with no obvious potential to translate to a functional protein; however, they regulate gene expression levels in the form of RNAs at a variety of levels (epigenetic, transcriptional and post-transcriptional regulations) (Kurokawa et al., 2009). Over the past decade, advances in genome-wide analysis of the eukaryotic transcriptome have revealed that up to 90% of the human genome are transcribed, however, GENCODE-annotated exons of protein-coding genes only cover 2.94% the genome, while the remaining are transcribed as non-coding RNAs (ncRNAs) (ENCODE Project Consortium, 2012). Non-coding transcripts are further divided into housekeeping ncRNAs and regulatory ncRNAs. Housekeeping ncRNAs, which are usually considered to be constitutive, include ribosomal, transfer, small nuclear and small nucleolar RNAs. Regulatory ncRNAs are generally divided into two classes based on nucleotide length. Those less than 200 nt are usually referred to as short/small ncRNAs, including microRNAs (miRNAs), small interfering RNAs and Piwi-associated RNAs, and those greater than

* Corresponding authors.
** Co-corresponding author.
E-mail addresses: 273352777@qq.com (C. Zhang), zh429@126.com (H. Zhang), whuili@163.com (H. Wang).

http://dx.doi.org/10.1016/j.aquatox.2016.12.003
0166-445X/

200 nt are known as long non-coding RNAs (lncRNAs) (Nagano and Fraser, 2011).

LncRNAs are involved in a variety of functions, including recruitment of chromatin remodelers and antisense regulation of messenger RNAs, serving as scaffolds for recruitment of regulatory proteins and sequestration of small regulatory RNAs (Trinarchi et al., 2014; Neguembor et al., 2014). Their involvement in the fundamental cellular processes including regulation of gene expression at epigenetics, transcription and post-transcription highlights a central role in cell homeostasis (Nakagawa and Kageyama, 2014). Since lncRNAs studies are still at a relatively early stage, their definition, conservation, functions and action mechanisms remain poorly understood. For example, when human hepatic epithelial (L-02) cells were exposed to arsenite, it resulted in increased lactate production, glucose consumption and expression of glycolysis-related genes (*HK-2*, *Eno-1* and *Glut-4*). This response might result from the over-expression of lncRNAs, metastasis-associated lung adenocarcinoma transcript 1, hypoxia inducible factors-α, and the transcriptional regulators of cellular response to hypoxia (Luo et al., 2016). Some lncRNAs can indirectly regulate physiological processes by means of miRNAs. For example, cigarette smoke extract (CSE) caused an altered cell cycle, increased lncRNA CCAT1 levels and decreased miR-218 levels in human bronchial epithelial (HBE) cells. Depletion of CCAT1 attenuated the CSE-induced decreases of miR-218 levels, suggesting that miR-218 is negatively regulated by CCAT1 in HBE cells exposed to CSE (Lu et al., 2016). In CCl_4-induced Sprague-Dawley rat liver fibrosis, H19 was significantly down-regulated in HSCs and fibrosis tissues, while an opposite pattern was observed for MeCP2 and IGF1R, suggesting that silencing of lncRNA-H19 can alter IGF1R over-expression (Yang et al., 2016). The altered lncRNA-HOTAIR and MALAT1 expression might be involved in response to polycyclic aromatic hydrocarbons-induced DNA damage (Gao et al., 2016). Another study found that lncRNAs response to radiation-induced DNA damage and oxidative stress was involved in the p53 signaling pathway (Nie et al., 2015). This suggests that lncRNAs-Loc554202 was significantly increased compared with normal control in breast cancer tissues, and associated with advanced pathologic stage and tumor size (Shi et al., 2014). However, to date, no data are available on the functions of lncRNAs in zebrafish when exposed to antibiotics.

Fluoroquinolones (FQs) and tetracyclines (TCs) are known as β-diketone antibiotics (DKAs) due to the presence of a diketone group in their molecular structure. The long-term use of FQs and TCs can result in immune toxicity, feminization, reproductive failure, abortion, *etc*. (Mulgaonkar et al., 2012). Our previous studies have confirmed the immunotoxicity and neurotoxicity of DKAs on zebrafish (Sheng et al., 2013). After a 3-month DKA exposure, transcriptome sequencing identified 10 differentially expressed genes among the genes related to KEGG pathways with high enrichment. Both detection of biomarkers and histopathological observation corroborated that chronic DKA exposure could result in abnormal expression of immune genes and enzymes, and variable levels of damage to immune related organs (Trapnell et al., 2013). DKAs also affected zebrafish movement behavior with a 6.25 mg/L treatment increasing zebrafish shoaling behavior (+38%), while 25 mg/L DKA exposure decreased zebrafish social cohesion (−41%). Additionally, the signal intensity of $^1O_2$ gradually decreased with increasing DKA concentration leading to insufficient energy supply and movement functional disorders (Mercer et al., 2009a).

Based on the above-mentioned toxicological effects of DKAs on zebrafish, we confirmed that the abnormalities in biomarkers, histopathology and behavior resulted from abnormal gene expression, and that these functional genes were mostly affected by regulation of lncRNAs. To date, no studies have examined the affected lncRNAs and their regulating target genes due to chronic DKA exposure. Therefore, this study aims to screen the regulation-related lncRNAs by means of high throughput sequencing technology, to analyze the differentially expressed lncRNAs from zebrafish (*Danio rerio*) following DKA exposure, and to predict the relative target genes for further *in vivo* verification of their abnormal changes. These results examine regulatory relationships between lncRNAs and their target genes, their related mechanisms, and probe the target point of drug action and their triggered diseases.

2. Materials and methods

2.1. Ethics statement

The use of zebrafish (*Danio rerio*) in this study was approved by Wenzhou Medical University's Institutional Animal Care and Use Committee (IACUC). All experiments were strictly performed following IACUC rules. All dissection was conducted on ice or specimens anesthetized with 0.03% tricaine (buffered MS-222) to decrease suffering.

2.2. Chemicals, fish husbandry and exposure protocols

Three FQs and three TCs were selected as representative DKA species: ofloxacin, ciprofloxacin, enrofloxacin, doxycycline, chlortetracycline and oxytetracycline. Purities were >99% except for chlortetracycline (95%). The six DKAs were gratis supplied by Amresco (Solon, OH, USA), and their structures are shown in Fig. S1. Wild-type (AB strain) zebrafish were raised in dechlorinated and filtered water (pH 6.5–7.5). Instant Ocean band of salt was added to raise the specific conductivity to 450–1000 μS/cm. Temperature was controlled at 28 °C and with a 14:10-h light/dark cycle (lights on at 8 a.m.) (Yu et al., 2008a). Zebrafish feeding and inspection of fertilized and normal embryos were conducted according to Kimmel and coworkers (Robinson et al., 2011). DKA-exposure concentrations were selected at 0, 6.25 (corresponding to 2.88, 3.14, 2.89, 2.03, 2.02 and 2.26 μmol/L for ofloxacin, ciprofloxacin, enrofloxacin, doxycycline, chlortetracycline and oxytetracycline, respectively) and 12.5 mg/L (corresponding to 5.76, 6.28, 5.79, 4.06, 4.04 and 4.52 μmol/L for ofloxacin, ciprofloxacin, enrofloxacin, doxycycline, chlortetracycline and oxytetracycline, respectively) of total DKAs with equal weight concentrations for each DKA species. At 6 dpf (days post fertilization), well-hatched zebrafish were transferred to 2 L tanks until 30 dpf. The DKA solution was renewed each day to maintain a constant DKA-exposure level (Liao et al., 2011). The control (survival rate >95%) and treatment groups were performed in triplicate. At 30 dpf, each group including control and treatments was transferred from 2 L to 12 L tanks. The DKA-exposure concentrations and daily DKA renewal frequency for the 12 L tanks were identical to those in the 2 L tanks.

2.3. Preparation of biological samples

After DKA exposure, zebrafish from three biological replicates were anesthetized with 0.03% tricaine (buffered MS-222). Each biological replicate included 9 zebrafish, and thus 27 zebrafish were used for RNA-seq, qRT-PCR and *in situ* hybridization observations. Concurrently, the liver and spleens were collected by dissection over ice.

2.4. Total RNA extraction and lncRNAs library construction

Zebrafish in control (0 mg/L) and treatment (6.25 and 12.5 mg/L) groups were randomly selected after DKA exposure at 90 dpf and rinsed with phosphorous buffer solution. The anatomy of the whole fish and total RNA extraction were characterized as detailed in our

previous report (Li et al., 2016a). After the quantity and purity of total RNA were determined, the rRNA was removed using a epicentre Ribo-Zero™ kit (Illumina Company, Madison, WI, USA) to recover and purify the remainder of the rRNA depleted RNA (polyA+ and polyA−). The recovered and purified rRNA depleted RNA was randomly broken into short segments by fragmentation buffer. Using the fragmented rRNA depleted RNA as a template, the first strand cDNA was synthesized by random hexamers. This step was followed by addition of buffer, dNTPs, RNaseH and DNA polymerase I to synthesize the second strand cDNA. The double-stranded product was purified by AMPure XP beads (Beckman Coulter, Shanghai, China), and the DNA cohesive ends were repaired to blunt-ends using T4 DNA polymerase and Klenow DNA polymerase activity. The 3′-end was added by the bases A and adapter, then fragments were selected by AMPureXP beads, followed by the degradation of the second strand cDNA containing U using enzyme USER. The final sequencing library was obtained by PCR amplification. After the library passed quality control inspection, we used an Illumina Hiseq 2000/2500 to sequence, and sequencing read length was double-ended to be 2 × 125 bp (PE125). The sequencing, evaluation and analysis of library quality were conducted on the basis of our previous report (Li et al., 2016a).

2.5. Identification of differentially expressed lncRNAs

Clean reads were mapped to the zebrafish genome using TopHat (http://tophat.cbcb.umd.edu/). Transcripts were assembled and annotated using the Cufflinks software package (http://cufflinks.cbcb.umd.edu/). TopHat and Cufflinks are free, open-source software tools for gene discovery and comprehensive expression analysis of high-throughput mRNA sequencing (RNAseq) data, which were jointly developed by Laboratory of Mathematics and Computer Biology, Berkeley, University of California and Laboratory of Barbara Wold, California Institute of Technology, California, USA. Together, they allowed biologists to identify new genes and new splice variants of known ones, as well as compared gene and transcript expression under two or more conditions (Trapnell et al., 2013). The known mRNAs were identified according to the latest annotation of the zebrafish genome sequence of Ensembl Danio rerio zv9.0 (ftp://ftp.Ensembl.org/pub/release-78/fasta/daniorerio/dna/). The remaining reads were filtered according to length and coding potentials, such that transcripts smaller than 200 bp were excluded and transcripts with CPC (Coding Potential Calculator) greater than −1 and CNCI (Coding Non-Coding Index) score greater than 0 were removed. The coding potential for the remaining transcripts was calculated by the Coding Potential Calculator based on quality, completeness, and sequence similarity of the open reading frame to proteins in the protein databases (Ewing and Green, 1998). The known protein-coding transcripts were identified.

Based on the above analytical results, the transcripts of candidate lncRNAs were cuffcompared with those of the known non-lncRNAs in zebrafish, and the same or similar transcripts were removed. Afterwards, the residual transcripts were cuffcompared with those of the known mRNAs, and the information on class code was counted. The transcripts for the five kinds of class codes were defined in detail as follows: (1) Unknown, intergenic transcript (u); (2) A transfrag falling entirely within a reference intron (i); (3) Exonic overlap with reference on the opposite strand (x); (4) Potentially novel isoform (fragment): at least one splice function is shared with a reference transcript (j); and (5) Generic exonic overlap with a reference transcript (o). The remaining unknown transcripts were used to screen for putative lncRNAs that met the following criteria: (1) lncRNA length ≥200 bp; (2) transcript reads coverage ≥3; and (3) exon number contained in transcript ≥1. All of the transcripts, which could satisfy the above requirements, were attributed to the finally novel lncRNAs. Expression levels for all transcripts, including putative lncRNAs and mRNAs, were quantified as FPKM using the Cuffdiff program from the Cufflinks package (Yao et al., 2010). Differential gene expression was determined using DESeq with a p-value <0.05 and a false discovery rate threshold of 5% (Trapnell et al., 2009).

2.6. Prediction of lncRNA functions

Functional identification of lncRNAs and mRNAs was performed according to co-expression and genomic co-location/required free energy for forming secondary structures between these differential lncRNAs and mRNAs. The regulation modes of lncRNAs were classified into two categories: (1) cis regulation, lncRNA's regulation for expression of their neighboring genes (the differentially expressed lncRNA and mRNA in the 100 kb range of chromosomes); and (2) trans regulation, lncRNA's regulation for expression of trans chromosome genes. Target genes for trans regulation were assessed mainly by the required free energy for forming secondary structures. The union of cis and trans regulation was considered to be the final target genes of lncRNAs.

2.7. Screening and qRT-PCR validation of differentially expressed lncRNAs and their target genes

In order to screen the differentially expressed lncRNAs, we reduced the search range of targets according to FPKM ≥ 50 and $|\log_2(\text{fold-change})| \geq 1$. The significant differentially expressed lncRNAs were found at the intersection of the three contrasting groups (6.25 mg/L *vs.* control, 12.5 mg/L *vs.* control, and 6.25 mg/L *vs.* 12.5 mg/L), which were further analyzed by Venn diagrams. The qRT-PCR operation and validation of the differentially expressed genes followed the methods of Li and coworkers (Li et al., 2016b). The amount of target molecules relative to the control was calculated by 2-ΔΔCt, and mRNA and lncRNA were expressed as fold-change according to the formula: $2-(\Delta Ct(\text{treated sample}) - \Delta Ct(\text{untreated sample}))$.

2.8. In situ *hybridization (ISH) and histopathological observation*

As shown in Supplementary Fig. S2, *in vitro* probe transcription demonstrated that both the lncRNA cloning and sequence alignment were correct (99–100%). Liver and spleen were collected by dissection from adult zebrafish exposed to DKAs from 4 hpf to 90 dpf. To further explore the spatial expression of lncRNAs in the spleen and liver of zebrafish, ISH was performed in 3 biological replicates (3 × 9, 9 zebrafish for each biological replicate), and each biological replicate was comprised of 3 technical replicates according to Yao et al. (2010). Probe synthesis was performed by *in vitro* transcription. Briefly, spleen and liver cryosections were prehybridized for 6 h at 65 °C with 700 μL prehybridization buffer (50% formamide, 5 × saline sodium citrate, 5 × Denhardt's, 200 μg/mL yeast RNA, 500 μg/mL salmon sperm DNA, 2% Roche blocking reagents, and diethylpyrocarbonate-treated water). The cryosections were then overlaid with 150 μL hybridization buffer (prehybridization buffer containing 1 pmol probes) and incubated overnight at 65 °C in a humidified chamber. After hybridization, the sections were washed 3 times with B1 buffer. The anti-digoxigenin-alkaline phosphatase fragments of antigen-binding fragments (Roche, Indianapolis, IN; 1:2500) and nitroblue tetrazolium and 5-bromo-4-chloro-3-indolyl phosphate (Promega) were used to detect the hybridization signals, which were quantified by Image-Pro Plus 6.0 Software (Media Cybemetics, Rockville, MD, USA). The isolated tissue treatments and HE staining were conducted using a standard protocol (Li et al., 2016b). Microscopic observation of tis-

sue damage was assessed using an optical microscope (DM2700 M, Leica, Germany).

2.9. Statistical analysis

The experimental data were reported as the mean ± SD (standard deviation). Each experimental group (0, 6.25 and 12.5 mg/L DKAs) contained three biological replicates, and each biological replicate was comprised of three technical replicates to assess accuracy and reproducibility. The number of zebrafish used in each biological replicate was 20 for qRT-PCR and 9 for ISH experiments. One-way ANOVA was performed to calculate statistical significance followed by post-hoc Dunnett tests to independently compare each DKA-exposure group to the control group. All statistical analyses were conducted with SPSS 18.0 (SPSS, Chicago, USA) using a $p < 0.05$ or $p < 0.01$ significance level, unless otherwise stated.

3. Results

3.1. High-throughput sequencing

Three cDNA libraries were constructed using mRNAs isolated from 0 (control), 6.25 and 12.5 mg/L DKA treatment groups, which were subsequently sequenced by an Illumina Hiseq2000/2500. This produced 27.62 gigabases (Gb) of valid reads, demonstrating that the sequencing data volume for each group was larger than 8 Gb. The deep sequencing produced 71,532,662 (control), 65,426,852 (6.25 mg/L treatment) and 84,020,924 (12.5 mg/L treatment) valid reads. To assess the quality of RNA-seq data, each base in the reads was assigned a quality score (Q) by a phred-like algorithm using FastQC (Derrien et al., 2012). Each sample's sequencing Q30 was higher than 99% indicating good sequencing quality (Table 1).

3.2. Identification and characterization of lncRNAs

We identified 16,602, 30,711 and 33,588 unique lncRNAs from the 0, 6.25 and 12.5 mg/L DKA treatment groups, respectively. According to the visible lncRNA levels in the three groups (Fig. 1A), we found that lncRNAs were evenly distributed across the 26 chromosomes of zebrafish with no obvious preference for location. Based on statistical categorization of lncRNAs into five class codes (Fig. 2), there were no lncRNAs in class code "i". In comparison, a high proportion (96.48%) of lncRNAs was found in class code "j" (51.7%) and "u" (44.8%) in control groups. However, the highest proportion occurred in class code "u", which accounted for 60.8% and 61.9% in the 6.25 and 12.5 mg/L treatment groups, respectively. These results demonstrated that the classes of alternative splicing events changed due to DKA exposure. Additionally, Fig. 1B indicates the distribution densities for the five classes of lncRNAs were different among different chromosomes. The distribution of antisense transcript code "x" in chromosomes was relatively even. In terms of lncRNA length, the majority of lncRNAs were relatively short. For example, more than 35% of lncRNAs were shorter than 300 nt, and more than 80% were shorter than 1000 nt. In contrast, the length distribution of mRNAs displayed an opposite trend compared to lncRNAs (Fig. 1C), *i.e.*, >68% of mRNAs were longer than 1100 bp.

3.3. Analyses of differentially expressed lncRNAs to DKA exposure

To identify DKA-responsive lncRNAs, the normalized expression (fragments per kilobase of exon per million fragments mapped, FPKM) of lncRNAs was compared among the three treatment libraries. We conducted a Volcano plot analysis for lncRNA overall distribution with the abscissa and ordinate representing $X = \log_2(\text{fold-change})$ and $Y = -\log_{10}(p\text{-value})$, respectively. The differentially expressed lncRNAs met the following criteria: $|X| \geq 1$ and

Table 1
The sequencing quality evaluation and statistical analyses.

Sample (mg/L)	Sequencing result quality						Reference genome in comparison with reads			Reference genome in comparison with region			Interval distribution of different gene expression value					
	Raw data read ($\times 10^7$)	Base	Valid data read ($\times 10^7$)	Base	Valid read (%)	Q30 (%)	GC (%)	Mapped reads ($\times 10^7$)	Unique mapped reads ($\times 10^7$)	Multi mapped reads ($\times 10^7$)	Exon	Intron	Inter-genic	0–0.1 FI	0.1–0.3 FI	0.3–3.57 FI	3.57–15 FI	15–60 FI	>60 FI
Control	7.23	9.04 G	7.15	8.94 G	98.87	96.24	48	2.78 (38.8%)	2.57 (36.0%)	0.20. (2.8%)	89.2%	7.7%	3.1%	63512 (72.0%)	1912 (2.2%)	6629 (7.5%)	6598 (7.5%)	4880 (5.5%)	4686 (5.3%)
6.25	6.63	8.28 G	6.54	8.18 G	98.76	95.61	46.50	3.60 (55.1%)	2.82 (43.1%)	0.78 (12.0%)	87.1%	7.9%	3.8%	48624 (55.1%)	1759 (2.0%)	9675 (11.0%)	12013 (13.6%)	5530 (6.3%)	10616 (12.0%)
12.5	8.51	10.63 G	8.40	10.50 G	98.77	87.29	44.50	4.56 (54.3%)	4.12 (49.1%)	0.44 (5.2%)	88.9%	7.9%	3.3%	46509 (52.7%)	1606 (1.8%)	10796 (12.2%)	12399 (14.1%)	5978 (6.8%)	10929 (12.4%)

Note: Raw data read: initial sequence reads quantity; Valid data read: reads quantity after quality check and trimming; Q30: percent of reads with accuracy rate over 99.9%; FI = FPKM interval.

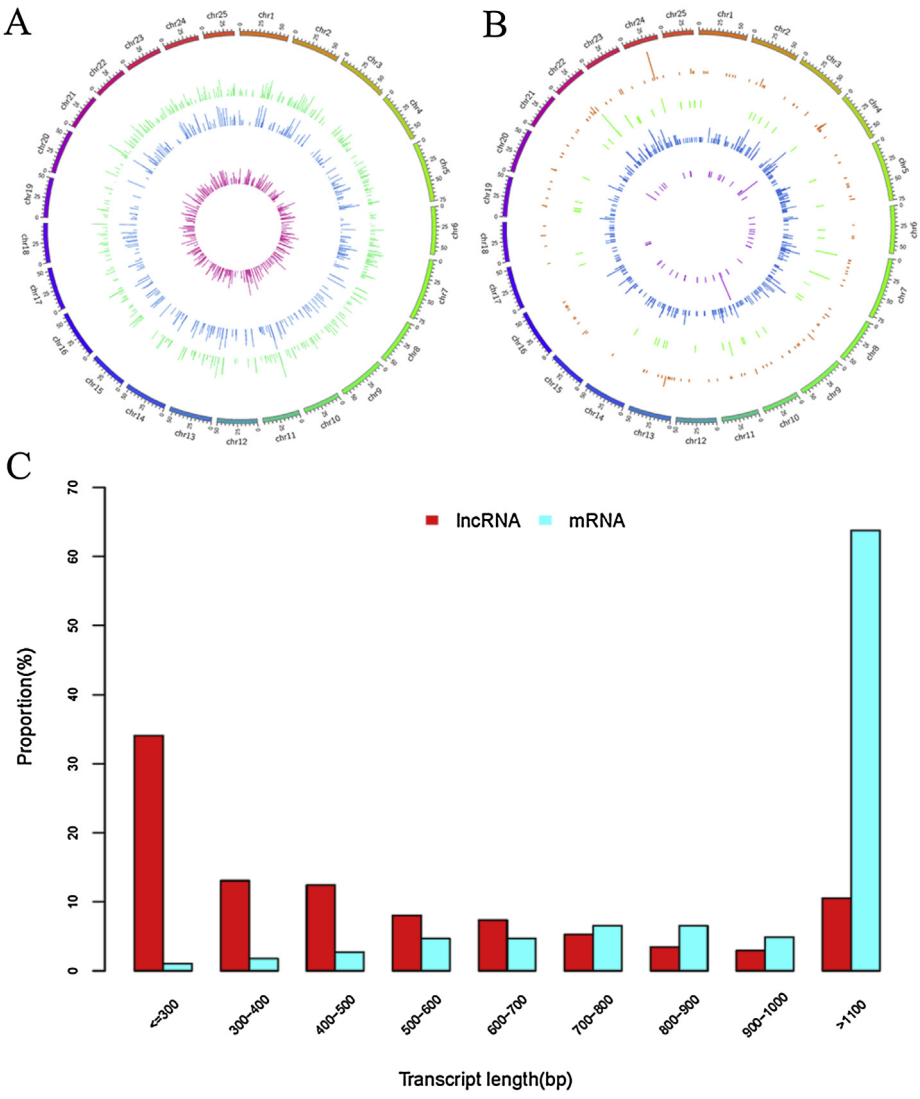

Fig. 1. The distribution characteristics of differentially expressed lncRNAs.
Note: A: The expression level of lncRNAs along the 26 zebrafish chromosomes. It comprises three concentric rings, which correspond to control, 6.25 mg/L and 12.5 mg/L treatment groups from outer to inner. B: Distribution of different types of lncRNAs. The different concentric rings from outer to inner represent code "o", "j", "x" and "u", respectively. C: Length distribution of lncRNAs and mRNAs.

$Y \geq -\log_{10}(0.05)$. The positive and negative values on the horizontal axis denote up-regulation and down-regulation, respectively. When compared with the control group, the 6.25 mg/L treatment led to up-regulation of 2064 lncRNAs and down-regulation of 778 lncRNAs. In contrast, the 12.5 mg/L treatment resulted in up-regulation of 2479 lncRNAs and down-regulation of 954 lncRNAs (Fig. 3A-B).

In order to increase the reliability of the differentially expressed lncRNAs, we screened out lncRNAs with high expression changes and high abundance. The DKA-responsive lncRNAs were identified by p-value ≤ 0.05, FPKM ≥ 50 and false discovery rate ≤ 0.05. The transcriptional levels of 44 lncRNAs in the 6.25 mg/L treatment and 39 lncRNAs in the 12.5 mg/L treatment were determined to be significantly changed by DKA exposure when compared to the control group. Venn diagrams showed common and specific lncRNAs whose expression was altered by DKA exposure. A total of 49 lncRNAs showed differential responses to the 6.25 and 12.5 mg/L treatments and the expression of 10 lncRNAs was changed in both 6.25 and 12.5 mg/L treatments (Fig. 3C). There are three kinds of modes for lncRNA-regulating target genes, *i.e.* local single chain structure (Gong and Maquat, 2011), local secondary structural motifs, and target molecular interaction of particular tertiary structural motifs (Gupta et al., 2010). Currently, it is difficult to acquire the tertiary structure of lncRNAs, while there is evidence for the regulation mechanism of lncRNA by local single chain and local secondary structure. As a result, analyses of the secondary structures of lncRNA target molecules are helpful to study their functional mechanisms, and further to probe the relationship between structures and functions of lncRNAs. At the same time, the lncRNAs with different secondary structures can exert different functions. For example, they can act as signal molecules to regulate downstream gene transcription, as decoy molecules to play a role in blocking molecules, as guide molecules to combine with proteins, or as scaffold molecules to accurately control signal transduction and molecular dynamics in multiple biological processes (Spitale et al., 2011). Therefore, the statistical analyses on the structural properties of 10 lncRNA sequences are helpful to reduce the amount of data in subsequent functional verification of lncRNAs and to increase our understanding to their regulation modes. In this investigation, the predicted secondary structures for 10 co-differentially expressed lncRNAs

Table 2
Information for 10 co-differentially expressed lncRNAs.

Test ID (TCONS_)	Class code	Gene ID (XLOC_)	Locus	Control (fpkm)	6.25 mg/L (fpkm)	12.5 mg/L (fpkm)	Sequencing length (bp)
00013798	u	008728	chr11:9612282-9612901	1240.82	0	0	206
00129029	u	083148	chr8:10932844-10935325	992.74	0	0	208
00011425	u	007033	chr11:6543405-6550766	821.43	0	0	204
00099955	u	063546	chr4:896459-899576	421.027	0	0	206
00092938	u	058975	chr3:60626805-60633302	344.502	0	0	213
00111658	u	071631	chr5:60459777-60460103	306.341	0	0	210
00027240	u	017599	chr14:32926917-32927286	283.721	0	0	265
00084041	u	053327	chr24:6180414-6180827	87.202	0	0	220
00011382	x	007003	chr11:6105995-6107000	72.6494	0	0	262
00017790	u	011347	chr12:50423620-50424538	0	72.52	93.33	226

Note: "u", Unknown, intergenic transcript; "x", Exonic overlap with reference on the opposite strand.

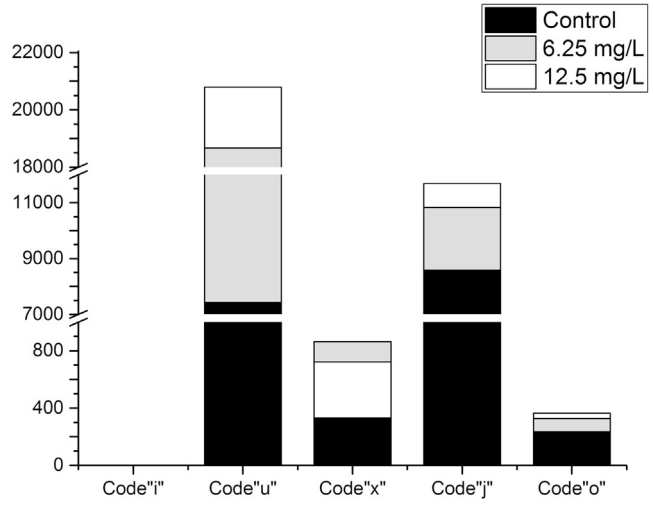

Fig. 2. Statistics of five kinds of lncRNA sequencing data.
Note: "u", Unknown, intergenic transcript (u); "i", A transfrag falling entirely within a reference intron (i); "x", Exonic overlap with reference on the opposite strand; "j", Potentially novel isoform (fragment): at least one splice function is hared with a reference transcript; "o", Generic exonic overlap with a reference transcript.

met the following criteria: (1) CPC; score <−1 and (2) CNCI score <0, as well as the previously-mentioned three criteria: (1) lncRNA length ≥200 bp; (2) transcript reads coverage; and (3) exon number contained in transcript ≥1 (Fig. 4). The information for the 10 co-differentially expressed lncRNAs is summarized in Table 2. Subsequently, we screened the differentially expressed target genes for each treatment group compared to the control group (Supplementary Table S1). The 10 screened lncRNAs and their target-gene putative interactive networks were constructed using Cytoscape 3.4 (Leroy Hood and Bruce laboratories). As demonstrated by Fig. 5, each lncRNA may regulate multiple target genes, and some target genes are regulated by a plurality of lncRNAs, therefore, constituting a complex regulatory network diagram.

3.4. Functional analyses of DKA-responsive lncRNAs

Previous studies showed that lncRNAs were preferentially located in close proximity to the genes they regulated (Rinn et al., 2007; Mercer et al., 2009b; Yu et al., 2008b; Campalans et al., 2004) and the required free energy was less than −30 to form secondary structures between lncRNA and mRNA. To reveal potential functions of the identified lncRNAs, we analyzed Gene Ontology (GO) terms for genes regulated by lncRNAs. Six significant enrichments ($p < 0.05$) and 12 GO terms were detected in zebrafish from the 6.25 and 12.5 mg/L treatment groups (Fig. 6). For example, GO term enrichments were found in molecular functions:

- GO:0004930, combining with an extracellular signal and transmitting the signal across the membrane by activating an associated G-protein;
- GO:0005509, interacting selectively and non-covalently with calcium ions (Ca^{2+});
- GO:0000166, interacting selectively and non-covalently with a nucleotide, any compound consisting of a nucleoside that is esterified with (ortho)phosphate or an oligophosphate at any hydroxyl group on the ribose or deoxyribose;

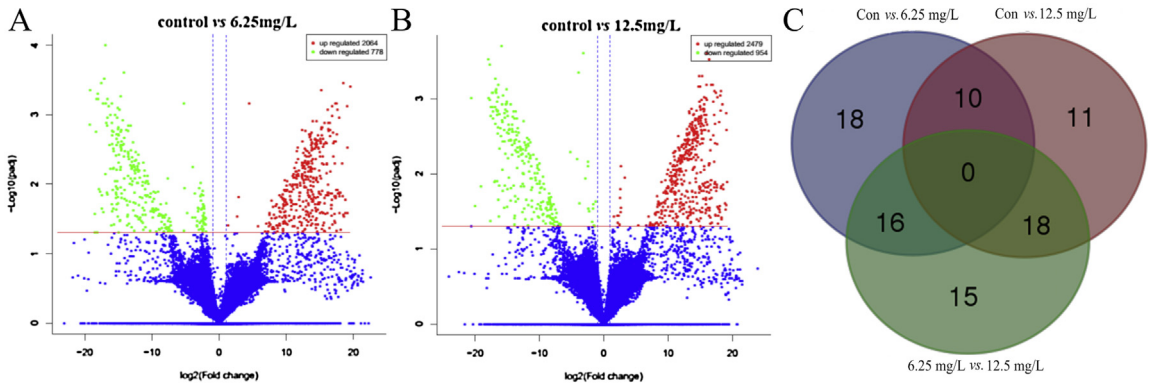

Fig. 3. Volcano and Venn diagrams of differentially expressed lncRNAs for the different comparison groups.
Note: (1) Abscissa represents $\log_2$(fold-change), and ordinate represents $-\log_{10}$(*p*-value); (2) Red dots denote the significant differentially expressed up-regulation lncRNAs; (3) Green dots denote the significant differentially expressed down-regulation lncRNAs; (4) Blue dots denote the non-significant differentially expressed lncRNAs; (5) A, Volcano diagram of lncRNAs between 6.25 mg/L treatment and control; (6) B, Volcano diagram of lncRNAs between 12.5 mg/L treatment and control; (7) C, Venn diagram of lncRNAs among control, 6.25 mg/L and 12.5 mg/L treatment groups.

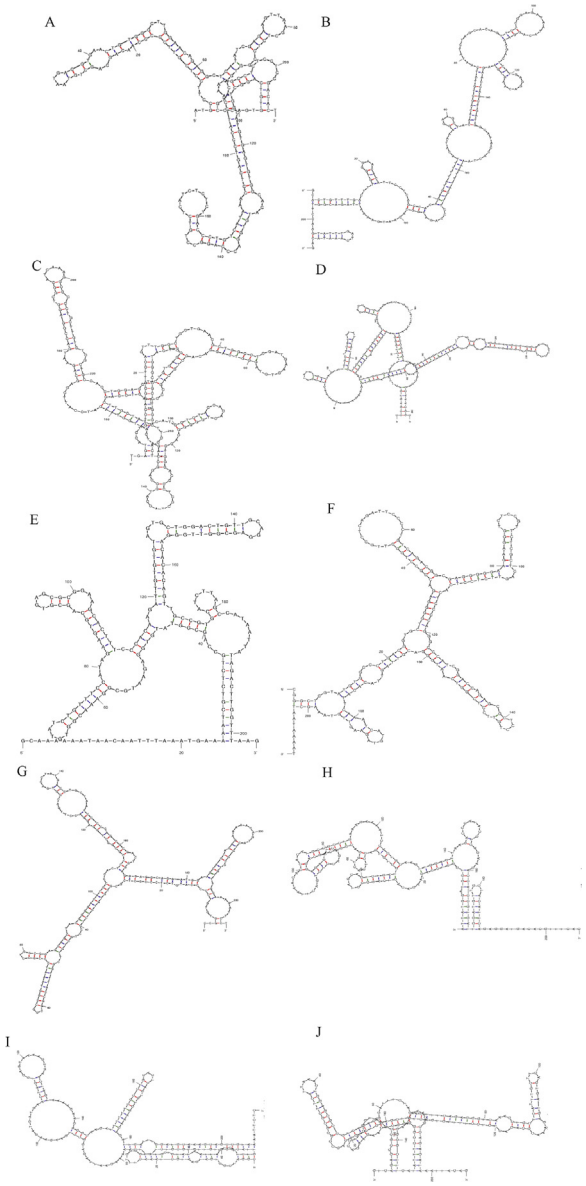

Fig. 4. Prediction of 10 candidate lncRNA secondary structures.
Note: A–J represents lncRNAs: TCONS_00129029, TCONS_00084041, TCONS_00027240, TCONS_00011382, TCONS_00011425, TCONS_00111658, TCONS_00017790, TCONS_00013798, TCONS_00092938 and TCONS_00099955.

- GO:0003723, interacting selectively and non-covalently with an RNA molecule or a portion thereof;
- GO:0020037, interacting selectively and non-covalently with heme, any compound of iron complexed in a porphyrin (tetrapyrrole) ring;
- GO:0005506, interacting selectively and non-covalently with iron ions and biological processes;
- GO:0006810, the directed movement of substances between cells by means of some agent such as a transporter or pore;
- GO:0007186, a series of molecular signals that proceeds with an activated receptor promoting the exchange of GDP for GTP on the alpha-subunit of an associated heterotrimeric G-protein complex;
- GO:0007155, the attachment of a cell, either to another cell or to an underlying substrate such as the extracellular matrix, *via* cell adhesion molecules;
- GO:0006886, the directed movement of proteins in a cell;
- GO:0006913, the directed movement of molecules between the nucleus and cytoplasm;
- GO:0007165, the cellular process in which a signal is conveyed to trigger a change in the activity or state of a cell.

These findings suggest that the DKA-responsive lncRNAs may regulate genes involved in many biological processes, including signal transduction, energy synthesis and transcription in response to DKA exposure.

3.5. Validation of co-differentially expressed lncRNAs and potential target genes

The qRT-PCR was used to verify 3 co-differentially expressed lncRNAs and their possible regulation genes. With increasing DKA-exposure concentrations, the expression of TCONS_00129029 and TCONS_00027240 decreased, but that of TCONS_00017790 increased (Fig. 7A). These trends for the 3 lncRNAs identified by high-throughput sequencing were consistent with those from qRT-PCR. We selected 7 potential target genes (*tenm3*, *smarcc1b*, *myo9ab*, *ubr4*, *hoxb3a*, *mycbp2* and *CR388046.3*), co-regulated by three lncRNAs (TCONS_00129029, TCONS_00027240 and TCONS_00017790), to analyze the consistency between their qRT-PCR and transcriptomic sequencing. The information for the above-mentioned 7 genes is listed in Supplementary Table S1. The consistent trends for the 7 target genes confirm the reliability of the sequencing results. Except for the *tenm3* and *smarcc1b* genes, the other 5 genes all showed up-regulation in the 6.25 mg/L treatment and but down-regulation in the 12.5 mg/L treatment (Fig. 7B).

3.6. Expression changes of candidate lncRNAs and target genes in different tissues by ISH

For the 3 lncRNAs (TCONS_00129029, TCONS_00027240 and TCONS_00017790), we explored their distribution and expression changes in zebrafish immune tissues (liver and spleen) by ISH. TCONS_00129029 showed high expression in the control group, while it decreased with increasing DKA-exposure concentrations in both liver and spleen. Similar expression of TCONS_00027240 occurred when compared with the control. In contrast, the expression of TCONS_00017790 in spleen tissue increased with increasing DKA-exposure concentrations (Fig. 8d), but the highest expression was observed in the 6.25 mg/L treatment group for liver tissue (Fig. 8b). According to the expression changes for the 3 lncRNAs in immune tissues, we speculated that the abnormal expression possibly affected regulation of zebrafish immune functions. Additionally, we screened out two immune-related possible target genes, *plk3* and *syt10*, which were simultaneously regulated by the 3 investigated lncRNAs. By ISH, a similar expression trend was observed for *plk3* and *syt10* in liver and spleen tissue, *i.e.*, *plk3* was inhibited in the 6.25 mg/L treatment group and expression increased in the 12.5 mg/L treatment group (Fig. 9a–d). In contrast, the expression of *syt10* was inhibited in both 6.25 and 12.5 mg/L treatments in the liver and spleen (Fig. 9a–d).

3.7. Tissue-section and histopathological analyses of liver and spleen

Histopathological observations on liver and spleen tissues were conducted with HE staining, and photographs of tissue damage were taken when the 3 biological replicates showed a high degree of uniformity. As shown in Fig. 10, hepatocytes in the control group had uniform nucleus and clear configuration, while in DKA-exposure groups they were reduced, swollen and vague, along with hepatic parenchyma vacuolar degeneration. Blood accumulation and clot formation were also noticed in DKA-exposed groups,

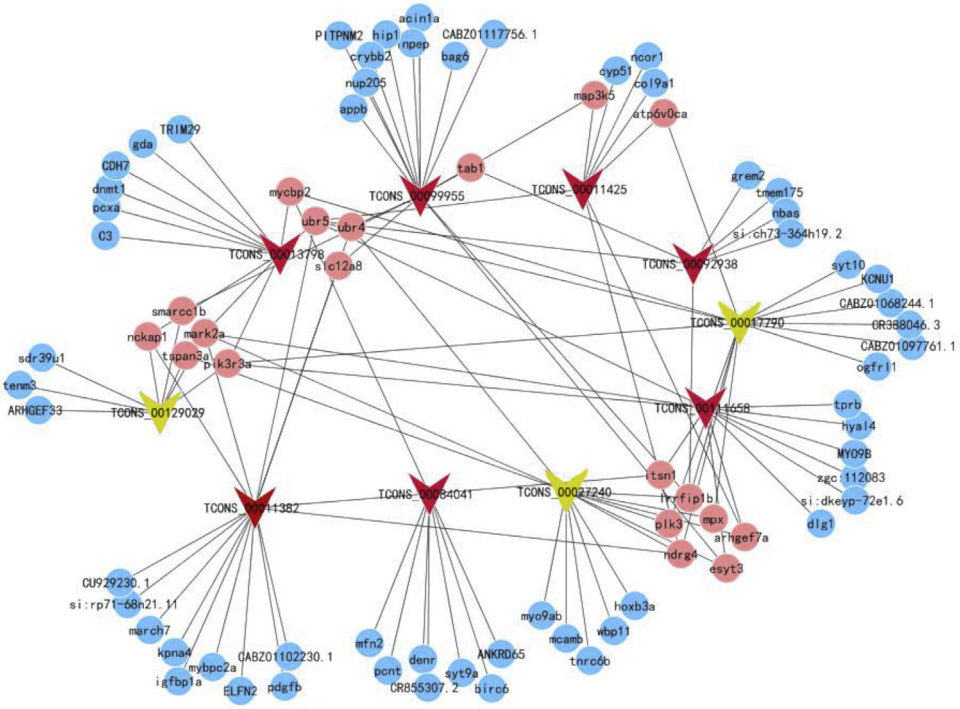

Fig. 5. Regulatory network of 10 candidate lncRNA and target genes.
Note: (1) A, the regulation network of 10 high-abundance lncRNAs (FPKM ≥ 50 and $|\log_2(\text{fold-change})| \geq 1$) and their related target genes; (2) The triangles denote lncRNAs; (3) The red balls indicate the target genes co-regulated by the 10 lncRNAs, and the blue balls indicate the target genes regulated by a single lncRNA; (4) The network diagram was plotted by Cytoscape (v3.3) software.

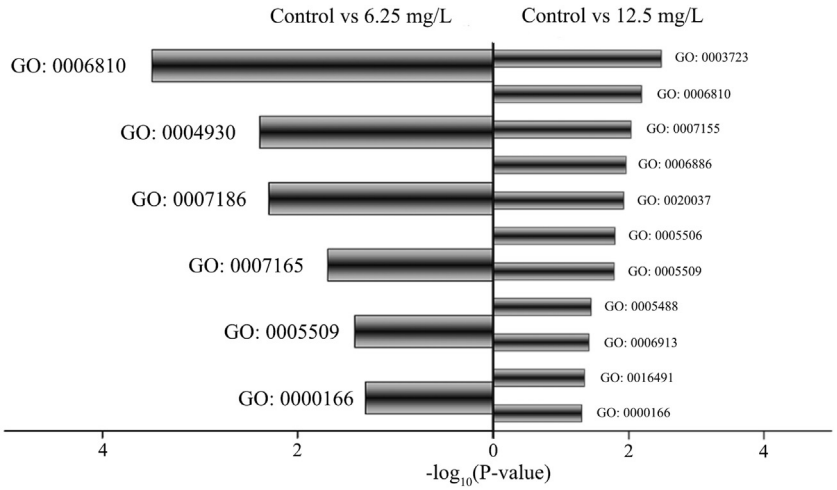

Fig. 6. GO functional enrichment analysis of the target genes regulated by the differentially expressed lncRNAs.
Note: (1) The X-axis indicates enrichment value on the basis of $-\log_{10}(P\text{-value})$; (2) The Y-axis represents GO term functions.

which was indicative of hepatic haemorrhagic lesion (Fig. 10A–C). For TCONS_00017790, the most effective binding target gene is TANK, which is reported as an associated NFKB activator (Tsuzuki et al., 2016). Under 200 × magnification, spleen cells in the control group were uniformly distributed and the cell structure was normal (Fig. 10D). In contrast, spleen cells were unevenly distributed, tissue structure was seriously damaged, and numerous brown metachromatic granules occurred in the 12.5 mg/L treatment group (Fig. 10F). Many cells became vague and indistinct, and the nucleus became larger in DKA-exposure treatments when compared to the control (Fig. 10E and F). This phenomenon may result from DKA-induced inflammation.

4. Discussion

The lncRNAs play important roles in many vital biological processes, emphasizing that they are not transcriptional "noise" (Wilusz et al., 2009). However, previous studies on lncRNAs in zebrafish are less extensive than in mammals. In zebrafish, previous reports mainly focused on protein-coding sequence changes in immune, nervous developmental processes under DKA exposure (Wang et al., 2016; Yin et al., 2014), but they did not assess changes of related genes from the perspective of lncRNA regulation. Ultimately, the expression changes of genes result from no-coding RNAs and transcriptional regulation. To further explore the mechanism for regulation and the biological effects from the

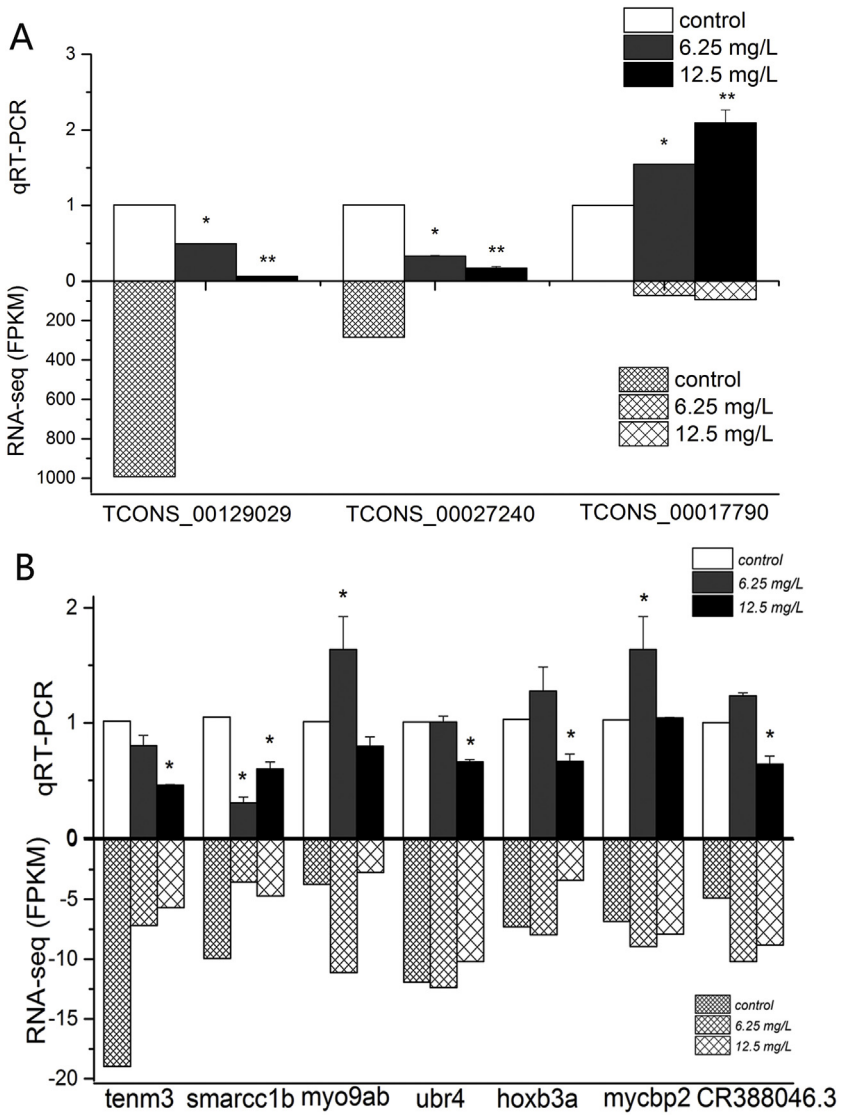

Fig. 7. The differential expression of candidate lncRNAs and target genes in the control and DKA-exposure treatment groups by qRT-PCR.
Note: A, RNA-seq and qRT-PCR of 3 lncRNAs; B, RNA-seq and qRT-PCR of 7 target genes co-regulated by the 3 lncRNAs.

expression changes of genes, we combined high-throughput RNA-seq with structural predication and functional analyses of lncRNAs. We found that lncRNAs were distributed throughout most the zebrafish genome, suggesting that lncRNA-coding regions are much more widespread than protein-coding regions (Fig. 1). Identification and characterization of a large number of lncRNAs in zebrafish provided valuable information for functional characterization of lncRNAs and post-transcriptional regulation mechanistic analyses, which were important for understanding the molecular targets and toxicological mechanisms resulting from DKA exposure.

The reverse transcription was conducted by means of complementary sequences of artificial adaptors to enrich lncRNAs with or without poly(A) tails. To distinguish sense from antisense lncRNAs, strand-specific libraries were constructed and paired-end sequencing was carried out. Our results identified different types of lncRNAs to facilitate functional studies. Moreover, the abundant original data generated in this study allow us to detect lncRNAs that have low expression levels. Given that the expression of lncRNAs was highly tissue-specific, we studied lncRNAs by ISH. This information is useful for predicting putative target organs and lncRNA-regulating target genes. Furthermore, we identified common and specific lncRNAs to study potential functions of differentially expressed lncRNAs in responses to DKA stress. To the best of our knowledge, this is the first comprehensive study of lncRNAs isolated from DKA-exposed zebrafish by means of high-throughput sequencing. Moreover, to assure that the putative lncRNAs conform to the criteria of length, structure and protein-coding ability, the putative lncRNAs were selected to have >200 bp in length and less than −1 for the coding potential score. These strict criteria and improved methods allowed us to identify lncRNAs with high sensitivity and selectivity.

Due to DKA exposure, expression changes of 3 lncRNAs (lncRNA-TCONS_00129029, TCONS_00027240 and TCONS_00017790) and their co-regulating target genes were confirmed in spleen and liver tissues by means of qRT-PCR and ISH. To date, little information is available for the above-mentioned lncRNAs and therefore the results of this study can enrich the functional database of lncRNAs. Based on previous immune toxicity research on DKAs by our group (Li et al., 2016a), the transcriptional changes demonstrated for *plk3* and *syt10* in this study appear to be associated with immune functions and are regulated by the above 3 lncRNAs. The histopathological observations further support our understanding of DKA response to immune toxicity mechanisms.

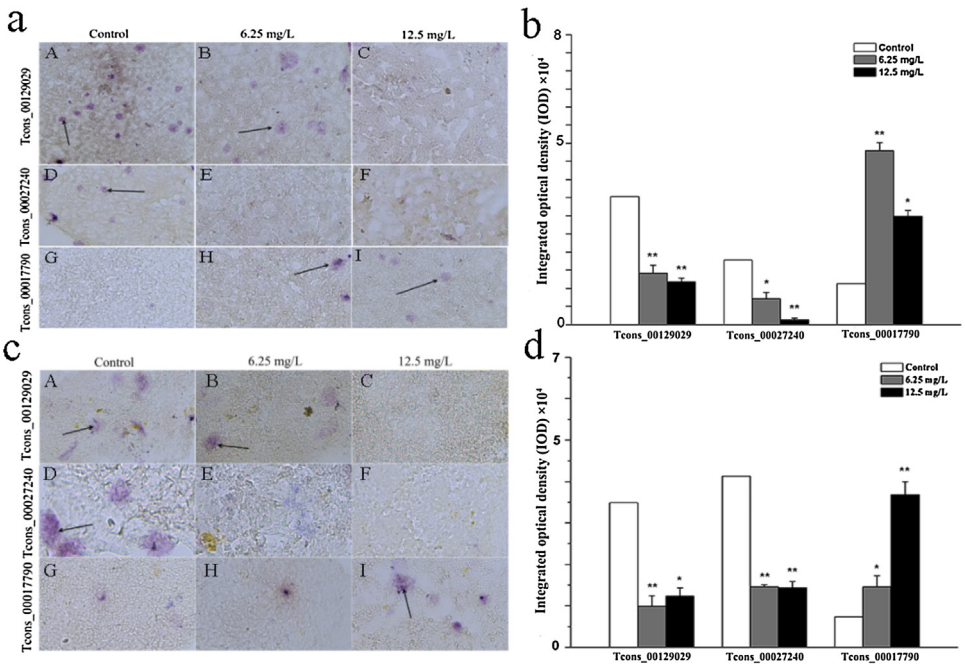

Fig. 8. The expression change of lncRNAs in liver and spleen induced by DKAs.
Note: (1) a, ISH of 3 lncRNAs expression in section of adult liver; (2) b, the relative fluorescence intensity units of 3 lncRNAs in adult liver; (3) c, ISH of 3 lncRNAs expression in section of adult spleen; (4) d, the relative fluorescence intensity units of 3 lncRNAs in adult spleen; (5) Arrow in Fig. 8a and 8c indicates ISH signal; (6) "*"and "**" in Fig. 8b and d indicate significance levels of $p < 0.05$ and $p < 0.01$, respectively; (7) All statistical analyses in Fig. 8 were performed by Dunnett tests.

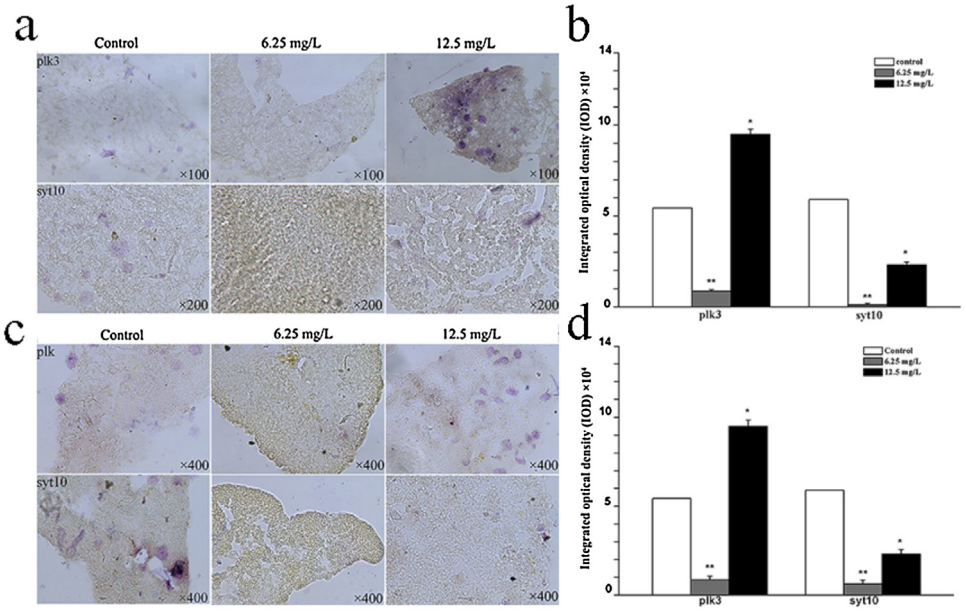

Fig. 9. The expression change of target genes in liver and spleen.
Note: Note: (1) a, ISH of *plk3* and *syt10* transcriptional levels, co-regulated by 3 lncRNAs, in section of adult liver; (2) b, the relative fluorescence intensity units of *plk3* and *syt10* in adult liver; (3) *c*, *ISH of plk3* and *syt10* transcriptional levels, co-regulated by 3 lncRNAs, in section of adult spleen; (4) d, the relative fluorescence intensity units of *plk3* and *syt10* in adult spleen; (5) "*" *and* "**" *in* Fig. 9b and d indicate significance levels of $p < 0.05$ and $p < 0.01$, respectively; (6) All statistical analyses in Fig. 9 were performed by Dunnett tests.

The *plk3* gene encodes new acidophilic kinases as it belongs to the Polo-like kinase (PLK) family that includes PLK1, PLK2 and PLK3 kinases. Although some progress has been made in deciphering the PLK1-dependent phosphoproteome, very little is known about the targets of PLK2 and PLK3 kinases. Salvi and coworkers (Salvi et al., 2012) identified and validated PLK2 and PLK3, new potential substrates HSP90, GRP-94, β-tubulin, calumenin, and 14-3-3 epsilon by means of 2-DE and mass spectrometry. The phosphosites generated by PLK3 in these proteins have been identified by mass spectrometry analysis providing new insights about PLKs specificity determinants (Fragoso and Barata, 2015). Recent evidence shows that PLK kinases could regulate the conformation, stability, homo- and heterotypic protein interactions, localization, and activity of the tumor suppressor PTEN (Wang et al., 2011). PLK3 was

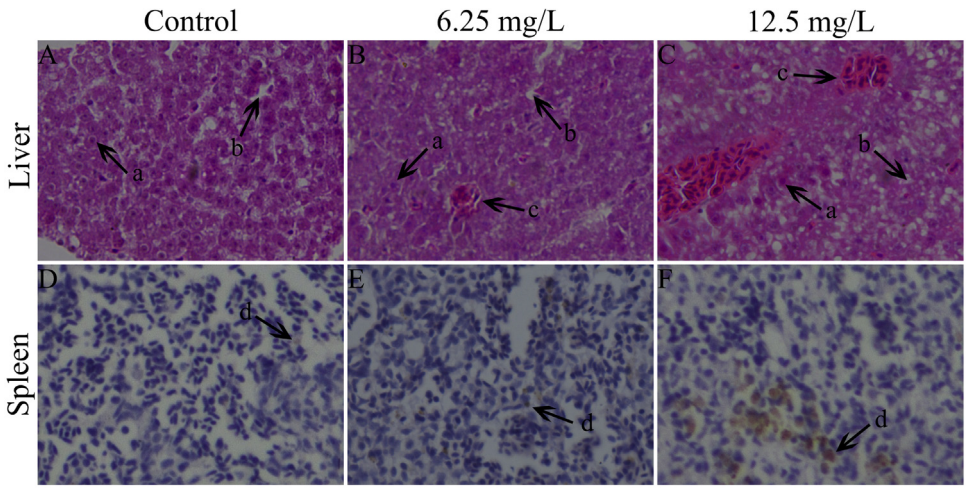

Fig. 10. HE dyeing of adult zebrafish hepatic and spleen tissues (200×).
Note: (1) A–C, hepatic tissue (200×); (2) D–F, spleen tissue (200×); (3) "a arrow" shows that DKA-exposure treatments lead to reduced, swollen and vague hepatocytes; (4) "b arrow" indicates that DKA-exposure treatments result in hepatic parenchyma vacuolar degeneration; (5) "c arrow" denotes that DKA-exposure treatments cause blood accumulated and clot formatted; and (6) "d arrow" denotes metachromatic granules.

implicated in Bcl-xL(Ser49) phosphorylation and is a downstream target associated with the cell G2 checkpoint, acting to stabilize G2 arrest. Bcl-xL phosphorylation at Ser49 also correlates with essential PLK3 activity and function, enabling cytokinesis and mitotic exit (Colwell et al., 2015). Prior work on *Synaptotagmin10 (syt10)* was mainly focused on nerve function, which came closest to SCN-specific genetic manipulation with the use of a *syt10* driver (Cao et al., 2011). *Syt10* functions as a Ca^{2+}-sensor that triggers IGF-1 exocytosis in neurons. Cao et al. (Macconachie et al., 2015) demonstrated that *syt10* controls a previously unrecognized pathway of Ca^{2+}-dependent exocytosis that is spatially and temporally distinct from Ca^{2+}-dependent synaptic vesicle exocytosis. The results of this study confirm that DKA exposure led to abnormal expression of *plk3* and *syt10* in spleen and liver tissues and histopathological injury. Thus our results support the inference that *plk3* and *syt10* were related to immune and endocrine functions.

5. Conclusions

In this study, we identified 16,602, 30,711 and 33,588 unique lncRNAs from three cDNA libraries. Of these lncRNAs, 44 and 39 were differentially expressed for the 6.25 mg/L and 12.5 mg/L treatment groups, respectively. Analysis of 12 GO terms for the target genes of the lncRNAs found that DKA-responsive lncRNAs might regulate genes involved in several biological processes, including signal transduction, energy synthesis and transcription. Complex interaction networks were constructed between lncRNAs and their target genes. Using qRT-PCR and ISH, we established that abnormal expression of TCONS_00129029, TCONS_00027240 and TCONS_00017790 in zebrafish liver and spleen tissues was due to the important role of lncRNAs in immune functions. Two immune-related target genes (*plk3* and *syt10*), co-regulated by the 3 identified lncRNAs above, were screened out, and a similar abnormal expression due to DKA exposure was found in both liver and spleen. Furthermore, DKA exposure caused a series of histopathological phenomena such as hepatic parenchyma vacuolar degeneration and brown metachromatic granules in spleen tissues. DKA exposure led to abnormal expression of some lncRNAs and their regulating target genes, which played an important regulation function in zebrafish immune tissues. These results can be used to further probe the interactions between lncRNAs and their target genes, and to analyze the functions of lncRNAs in resistance to environmental stress.

Acknowledgements

This work is jointly supported by the National Natural Science Foundation of China (31270548), the Natural Science Foundation and Public Beneficial Project of Zhejiang Province (LY17C030004 and 2016C34011), the Zhejiang Provincial Xinmiao Talent Project (2016R413005) and the Public Beneficial Project of Wenzhou City Sci & Technol Bureau (H20150005 and Y20150001).

Appendix A. Supplementary data

Supplementary data associated with this article can be found, in the online version, at http://dx.doi.org/10.1016/j.aquatox.2016.12.003.

References

Campalans, A., Kondorosi, A., Crespi, M., 2004. Enod40, a short open reading frame containing mRNA, induces cytoplasmic localization of a nuclear RNA binding protein in Medicago truncatula. Plant Cell 16, 1047–1059.
Cao, P., Maximov, A., Sudhof, T.C., 2011. Activity-dependent IGF-1 exocytosis is controlled by the Ca^{2+}-sensor synaptotagmin-10. Cell 145, 300–311.
Colwell, C.S., Kudo, T., Loh, D.H., 2015. Short circuiting the circadian system with a new generation of precision tools. Neuron 85, 895–898.
Derrien, T., Johnson, R., Bussotti, G., Tanzer, A., Djebali, S., Tilgner, H., 2012. The GENCODE v7 catalog of human long noncoding RNAs: analysis of their gene structure, evolution, and expression. Genome Res. 22, 1775–1789.
ENCODE Project Consortium, 2012. An integrated encyclopedia of DNA. Elements in the human genome. Nature 489, 57–74.
Ewing, B., Green, P., 1998. Base-calling of automated sequencer traces using phred. II. Error probabilities. Genome Res. 8, 186–194.
Fragoso, R., Barata, J.T., 2015. Kinases: tails and more: regulation of PTEN function by phosphorylation. Methods 77–78, 75–81.
Gao, C., He, Z.N., Li, J., Li, X., Bai, Q., 2016. Specific long non-coding RNAs response to occupational PAHs exposure in coke oven workers. Toxicol. Rep. 3, 160–166.
Gong, C., Maquat, L.E., 2011. lncRNAs transactivate STAU1-mediated mRNA decay by duplexing with 3 [prime] UTRs via Alu elements. Nature 470, 284–288.
Gupta, R.A., Shah, N., Wang, K.C., 2010. Long non-codingRN HOTAIR reprograms chromatin state to promote cancer metastasis. Nature 464, 1071–1076.
Kurokawa, R., Rosenfeld, M.G., Glass, C.K., 2009. Transcriptional regulation through noncoding RNAs and epigenetic modifications. RNA Biol. 6, 233–236.
Li, F.H., Wang, H., Liu, J.F., Wang, X.D., Wang, H.L., 2016a. Immunotoxicity of β-diketone antibiotic mixtures to zebrafish (*Danio rerio*) by transcriptome analysis. PLoS One 11, e0152530.
Li, J.Y., Zhang, Y.H., Wang, X.D., Li, W.J., Zhang, H.Q., Wang, H.L., 2016b. Screening on the differentially expressed miRNAs in zebrafish (*Danio rerio*) exposed to trace diketone antibiotics and their related functions. Aquat. Toxicol. 178, 27–38.
Liao, Q., Liu, C.N., Yuan, X.Y., Kang, S.L., Miao, R.Y., Xiao, H., 2011. Large-scale prediction of long non-coding RNA functions in a non-coding gene co-expression network. Nucleic Acids Res. 39, 3864–3878.

Lu, L., Xu, H., Luo, F., Liu, X.L., Lu, X.L., 2016. Epigenetic silencing of miR-218 by the lncRNA CCAT1, acting via BMI1, promotes an altered cell cycle transition in the malignant transformation of HBE cells induced by cigarette smoke extract. Toxicol. Appl. Pharm. 304, 30–41.
Luo, F., Liu, X.L., Ling, M., Lu, L., Shi, L., 2016. The lncRNA MALAT1, acting through HIF-1α stabilization, enhances arsenite-induced glycolysis in human hepatic L-02 cells. BBA Mol. Basis Dis. 1862, 1685–1695.
Macconachie, L.P., Poyiadji, N.C., Rao, T.C., Anantharam, A., 2015. The membrane bending action of the Syt-1 C2AB studied on supported lipid bilayers. Cell Biophys. J. 108, 104–109.
Mercer, T.R., Dinger, M.E., Mattick, J.S., 2009a. Long non-coding RNAs: insights into functions. Nat. Rev. Genet. 10, 155–159.
Mercer, T.R., Dinger, M.E., Mattick, J.S., 2009b. Long non-coding RNAs: insights into functions. Nat. Rev. Genet. 10, 155–159.
Mulgaonkar, A., Venitz, J., Sweet, D., 2012. Fluoroquinolone disposition: identification of the contribution of renal secretory and reabsorptive drug transporters. Expert Opin. Drug Met. 8, 553–559.
Nagano, T., Fraser, P., 2011. No-nonsense functions for long noncoding RNAs. Cell 145, 178–181.
Nakagawa, S., Kageyama, Y., 2014. Nuclear lncRNAs as epigenetic regulators-beyond skepticism. BBA Gene Regul. Mech. 1839, 215–222.
Neguembor, M.V., Jothi, M., Gabellini, D., 2014. Long noncoding RNAs, emerging players in muscle differentiation and disease. Skelet. Muscle 4, 8–14.
Nie, J.H., Peng, C.J., Pei, W.W., Zhu, W., Zhang, S.Y., 2015. A novel role of long non-coding RNAs in response to X-ray irradiation. Toxicol. In Vitro 30, 536–544.
Rinn, J.L., Kertesz, M., Wang, J.K., Squazzo, S.L., Xu, X., Brugmann, S.A., 2007. Functional demarcation of active and silent chromatin domains in human HOX loci by noncoding RNAs. Cell 129, 1311–1323.
Robinson, J.T., Thorvaldsdottir, H., Winckler, W., Guttman, M., Lander, E.S., Getz, G., 2011. Integrative genomics viewer. Nat. Biotechnol. 29, 24–36.
Salvi, M., Trashi, E., Cozza, G., Franchin, C., Arrigoni, G., 2012. Investigation on PLK2 and PLK3 substrate recognition. BBA Proteins Proteomics 1824, 1366–1373.
Sheng, Z.G., Huang, W., Liu, Y.X., Yuan, Y., Zhu, B.Z., 2013. Ofloxacin induces apoptosis via (1 integrin-EGFR-Rac1-Nox2 pathway in microencapsulated chondrocytes. Toxicol. Appl. Pharmacol. 267, 74–87.
Shi, Y.G., Lu, J.W., Zhou, J., Tan, X.M., Ye, H., 2014. Long non-coding RNA Loc554202 regulates proliferation and migration in breast cancer cells. Biochem. Biophys. Res. Commun. 446, 448–453.
Soshnev, A.A., Ishimoto, H., McAllister, B.F., Li, X., Wehling, M.D., Kitamoto, T., 2011. A conserved long noncoding RNA affects sleep behavior in Drosophila. Genetics 189, 455–468.
Spitale, R.C., Tsai, M.C., Chang, H.Y., 2011. RNA templating the epigenome long noncoding RNAs as molecular scaffolds. Epigenetics 6, 539–543.
Trapnell, C., Pachter, L., Salzberg, S.L., 2009. TopHat: discovering splice junctions with RNA-Seq. Bioinformatics 25, 1105–1111.
Trapnell, C., Roberts, A., Goff, L., Pertea, G., Kim, D., Kelley, D.R., Pimentel, H., Salzberg, S.L., Rinn, J.L., Pachter, L., 2013. Differential gene and transcript expression analysis of RNA-seq experiments with TopHat and Cufflinks. Nat. Protoc. 7 (3), 562–578.
Trinarchi, T., Bilal, E., Ntziachristos, P., Fabbri, G., Dalla-Favera, R., 2014. Genome-wide mapping and characterization of notch-regulated long noncoding RNAs in acute Leukemia. Cell 158, 593–606.
Tsuzuki, S., Tachibana, M., Hemmi, M., Yamaguchi, T., Shoji, M., Sakurai, F., Kobiyama, K., Kawabata, K., Ishii, K.J., Akira, S., Mizuguchi, H., 2016. TANK-binding kinase 1-dependent or −independent signaling elicits the cell-type-specific innate immune responses induced by the adenovirus vector. Int. Immunol. 28, 105–115.
Wang, J.F., Beauchemin, M., Bertrand, R., 2011. Bcl-xL phosphorylation at Ser49 by polo kinase 3 during cell cycle progression and checkpoints. Cell Signal. 23, 2030–2038.
Wang, X.D., Zheng, Y.S., Zhang, Y.N., Wang, H.L., 2016. Effects of β-diketone antibiotic mixtures on behavior of zebrafish (*Danio rerio*). Chemosphere 144, 2195–2205.
Wilusz, J.E., Sunwoo, H., Spector, D.L., 2009. Long noncoding RNAs: functional surprises from the RNA world. Gene Dev. 23, 1494–1504.
Yan, B., Wang, Z.H., Guo, J.T., 2012. The research strategies for probing the function of long noncoding RNAs. Genomics 99, 76–80.
Yang, J.J., Liu, L.P., Tao, H., Hu, W., Shi, P., Deng, Z.Y., Li, J., 2016. MeCP2 silencing of LncRNA H19 controls hepatic stellate cell proliferation by targeting IGF1R. Toxicology 359–360, 39–46.
Yao, G., Yin, M., Lian, J., Tian, H., Liu, L., Li, X., Sun, F., 2010. microRNA-224 is involved in transforming growth factor-beta-mediated mouse granulosa cell proliferation and granulosa cell function by targeting Smad4. Mol. Endocrinol. 24, 540–551.
Yin, X.H., Wang, H.L., Zhang, Y.N., Dahlgren, R.A., Zhang, H.Q., Shi, M.R., Wang, X.D., 2014. Toxicological assessment of trace β-diketone antibiotic mixtures on zebrafish (*Danio rerio*) by proteomic analysis. PLoS One 9, e102731.
Yu, W.Q., Gius, D., Onyango, P., Muldoon-Jacobs, K., Karp, J., Feinberg, A.P., 2008a. Epigenetic silencing of tumour suppressor gene p15 by its antisense RNA. Nature 451, 202–206.
Yu, W.Q., Gius, D., Onyango, P., Muldoon-Jacobs, K., Karp, J., Feinberg, A.P., 2008b. Epigenetic silencing of tumour suppressor gene p15 by its antisense RNA. Nature 451, 202–206.